Attraction between like-charged surfaces induced by orientational ordering of divalent rigid rod-like counterions: theory and simulations

2009 J. Phys. A: Math. Theor. 42 105401

(http://iopscience.iop.org/1751-8121/42/10/105401)

IOP PUBLISHING JOURNAL OF PHYSICS A: MATHEMATICAL AND THEORETICAL

J. Phys. A: Math. Theor. **42** (2009) 105401 (14pp) doi:10.1088/1751-8113/42/10/105401

Attraction between like-charged surfaces induced by orientational ordering of divalent rigid rod-like counterions: theory and simulations

Stefano Maset[1], **Jurij Reščič**[2], **Sylvio May**[3], **Janez Ivan Pavlič**[4,5] **and Klemen Bohinc**[4,5,6]

[1] Department of Mathematics and Informatics, University of Trieste, Trieste, Italy
[2] Faculty of Chemistry and Chemical Technology, University of Ljubljana, Ljubljana, Slovenia
[3] Department of Physics, North Dakota State University, Fargo, North Dakota, USA
[4] College of Health Studies, University of Ljubljana, Ljubljana, Slovenia
[5] Laboratory of Physics, Faculty of Electrical Engineering, University of Ljubljana, Ljubljana, Slovenia

E-mail: klemen.bohinc@fe.uni-lj.si

Received 20 October 2008
Published 13 February 2009
Online at stacks.iop.org/JPhysA/42/105401

Abstract

We consider the interaction between two equally charged surfaces in an electrolyte solution composed of long divalent rigid rod-like counterions of arbitrary length. Further, we study the influence of orientational ordering of rigid rod-like counterions on the interaction between charged surfaces. Density functional theory is introduced, where the spatial distribution of charge within the divalent rod-like counterions is represented by two effective charges at a fixed distance. The result of variational procedure gives an integral differential equation for the electrostatic potential which was solved numerically. From the electrostatic potential and the concentration of counterions, the free energy of two charged surfaces interacting in a solution of rod-like counterions is calculated. For large surface charge densities and for long enough divalent rod-like counterions the minimum of the free energy is obtained at a distance between the surfaces which equals the counterion length. This indicates that a bridging mechanism might be responsible for the attraction between like-charged surfaces. The analysis of the orientational distribution function confirms that, at the minimum of the free energy, the rod-like counterions are oriented perpendicularly and thus connect the like-charged surfaces. Finally, canonical Monte-Carlo simulations confirm the theoretical calculations of the osmotic pressure between like-charged surfaces for long enough rod-like counterions.

PACS numbers: 41.20.Cv, 46.70.Hg

[6] Author to whom any correspondence should be addressed.

1. Introduction

Electrostatic interactions between strongly charged objects (macroions) in aqueous solutions play an important role in chemistry, biology and technology [1]. Usually the macroions appear as charged surfaces of mica, charged lipid membranes, DNA, colloids, actin molecules, proteins, viruses and even cells. The intervening solution always contains simple salt and often also multivalent ions. The role of multivalent ions in the solution can be played by multivalent metal ions, dendrimers, charged micelles, polyelectrolytes including DNA and polyamines.

Mean-field electrostatic theory predicts purely repulsive interaction between like-charged colloidal particles. However, a growing number of experimental observations where multivalent ions were involved, have challenged its validity. During the last decade computer simulations provided detailed insight into mechanisms which lead to attractions between like-charged colloidal particles [2, 3].

In biology, there are many phenomena that motivate studies of electrostatic effects between macroions in solution. Condensation of DNA is induced by the presence of multivalent counterions [4, 5] which is relevant, for example, for the packing of DNA in viruses. The complexation of DNA with positively charged proteins underlies chromatin structure, that with positively charged membranes leads to lipoplex formation [6, 7]. Network formation in actin solutions [8] is the consequence of the attractive interactions between cytoskeletal filamentous actin molecules mediated by multivalent ions. The aggregation of rod-like M13 viruses is induced by divalent tunable diamin ions [9].

Experimentally, the swelling of the lamellar liquid crystalline phase within a solution composed of monovalent or divalent ions [10] was studied. It was shown that replacing monovalent counterions with divalent ones drastically decreases swelling of lamellar phases [11]. Short-range attractions between equally charged mica or clay surfaces in a solution of divalent ions have been detected in direct surface force measurements and atomic force microscopy [12].

Mean-field Poisson–Boltzmann theory does not predict attraction between equally charged surfaces [13]. Hence, attraction must be caused by charge–charge correlations. Indeed, accounting for inter-ionic correlations between (multivalent) counterions and charged surfaces leads to the possibility of attractive force [14–16]. The Monte-Carlo (MC) simulations of Guldbrand *et al* [17] first confirmed the existence of attraction between equally charged surfaces immersed into a solution composed of divalent ions in the limit of high surface charge density. These and other MC simulations [18–20] showed that attractive interactions between equally charged surfaces may arise for high surface charge density, low temperature, low relative permittivity and polyvalent counterions. Various other theoretical approaches aim at characterizing the role of inter-ionic correlations [19, 21–23]. Among these is the anisotropic hypernetted chain approximation within the primitive electrolyte model which was applied to divalent ions where each ion was modeled as a charged hard sphere immersed in a continuum dielectric medium [24–26]. At moderate distances between the (equally) charged surfaces and high surface charge densities attraction was observed. A key concept in interpreting the origin of the attraction comes from Rouzina *et al* [27] who suggested that at sufficiently low temperature the counterions should form two-dimensional Wigner crystals on each surface which upon close approach to the surfaces become inter-locked and thus mediate attraction. However, Linse has shown that correlation attraction occurs even if no Wigner crystal arrangement is present [28].

The force between two equally charged surfaces in the presence of polyelectrolytes was also studied [29, 30]. These studies showed that the strong attractive forces between charged surfaces were the result of the stretching of chains spanning the slit between the surfaces—the

so-called bridging [31]. It is strongest at a surface separation equal to an average monomer–monomer bond length [29]. These studies were extended to account for the presence of a simple salt of monovalent ions [32]. Most theoretical studies and Monte-Carlo simulations [29–31] have been concerned with flexible chains, but semi-flexible chains have also been introduced [33]. Recently, Turesson *et al* [34] have considered stiff polyelectrolytes and their role in the inter-surface interactions. They showed that in the limit of infinitely stiff chains, the bridging attraction is lost and is replaced by a strong correlation attraction, at short distances.

Another possibility for the appearance of attractive interactions between like-charged surfaces originates in the internal structure of multivalent ions. Here, individual charges within an ion are spatially separated through non-electrostatic interactions such as steric constraints [35–37]. In this case, intra-ionic correlations add to the presence of inter-ionic ones. In fact, intra-ionic correlations alone are sufficient to change repulsive into attractive interactions. A simple and generic case of multivalent ions that bear an internal structure are rod-like ions that carry a single charge on each end. As was shown recently [35] mean-field electrostatic theory with incorporated intra-ionic correlations can principally predict attraction between like-charged planar surfaces for such divalent rod-like ions. More, specifically, the study of Bohinc *et al* [35] was based on a series expansion of the ionic densities in the system in terms of the rod length l. In another study [38], an integral differential equation was derived for the same system (a mixture of positively and negatively charged divalent rod-like ions) for arbitrary rod-length l.

We note that in both previous approaches [35, 38] a mixture of positively and negatively charged divalent rod-like ions was considered. Typically, there will be only one rod-like ionic species (as is the case, for example, in the condensation of DNA by spermine or spermidine). It should therefore be of principal interest to consider two charged surfaces with only rod-like counterions between them (that is, no other ionic species). Here, no constant screening length exists and we expect the minimal rod-length necessary to mediate attraction to depend on the charge density of the two surfaces. The presentation of the numerical method and results for this relationship is the subject of the present work. We derive an integral differential equation which predicts the spatial and orientational ionic distributions for rod-like multivalent counterions of arbitrary length. Restrictions of the orientational degrees of freedom near the hard charged surfaces are taken into account. We also compare our solutions of the integral differential equation with Monte-Carlo simulations. The comparison supports our notion that with growing rod-length the importance of inter-ionic correlations decreases and our density functional theory becomes increasingly appropriate. We calculate the free energy of the system and the osmotic pressure between like-charged surfaces and show that both procedures predict the same energetically most favorable distance between like-charged surfaces.

2. Model and methods

2.1. Model

We consider an aqueous solution containing one single species of multivalent rod-like ions (figure 1). Each rod-like ion consists of two identical positive charges of valency Z, separated by a fixed distance l. In our model the ionic solution is sandwiched between two large, planar surfaces of surface area A (figure 1), each carrying a uniform average negative surface charge density σ. Clearly, the rod-like ions serve as counterions of the oppositely charged planar macroions. The distance between the two surfaces of the macroions is denoted by D. In the present study, we focus specifically on the case $Z = 1$.

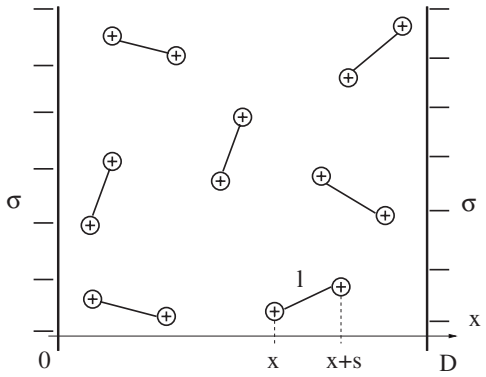

Figure 1. Schematic illustration of two like-charged planar surfaces with surface charge density σ interacting in a solution containing multivalent rod-like counterions. Each rod-like ion has two point charges Ze separated by a fixed distance l. For one particular ion the two locations of the two charges, x and $x + s$ are indicated.

In our theory the electrostatic field of the system varies only along the x-axis, the normal direction between the two charged surfaces. We assume that there is no electric field behind each of the two charged planar surfaces (which is appropriate if inside the macroions the dielectric constant is much smaller than in the aqueous region between the surfaces). Rod-like counterions are characterized by positional and orientational degrees of freedom. We describe them by referring to one of the two charges of each particle as a reference charge, denoting the local concentration of all the reference charges by $n(x)$. The location of the second charge of a given counterion is then specified by the conditional probability density $p(s|x)$, denoting the probability to find the second charge at position $x + s$ if the first resides at x. At any given position x, we require the normalization condition

$$\frac{1}{2l}\int_{-l}^{l} \mathrm{d}s\; p(s|x) = 1 \tag{1}$$

to be fulfilled. Note also that $p(s|x) = 0$ for $|s| > l$.

2.2. Theory

The Helmholtz free energy of the system, measured per unit area of the surface and divided by the thermal energy unit, kT, consists of three terms: electrostatic energy, as well as translational and orientational entropy of the multivalent rod-like particles,

$$\frac{F}{AkT} = \frac{1}{8\pi l_B}\int_0^D \mathrm{d}x\; \Psi'(x)^2 + \int_0^D \mathrm{d}x[n(x)\ln[\lambda n(x)] - n(x)] + \int_0^D \mathrm{d}x\, n(x)\frac{1}{2l}\int_{-l}^{l} \mathrm{d}s\; p(s|x)[\ln p(s|x) + U(x,s)]. \tag{2}$$

Here the electrostatic potential, $\phi(x)$ is expressed in terms of the reduced (dimensionless) electrostatic potential, $\Psi = e\phi(x)/kT$, where e is the elementary charge. Also, as a measure of the dielectric constant within the aqueous solution ϵ we use the Bjerrum length $l_\mathrm{B} = e^2/4\pi\epsilon\epsilon_0 kT$ where ϵ_0 is the permittivity in vacuum. Note that the constant λ can be chosen so as to ensure overall charge neutrality in the system (it is thus not required to introduce this constraint explicitly). Finally, the function $U(x, s)$ can generally be viewed as

a non-electrostatic potential that acts on the rod-like ions and depends both on location and orientation. In our specific case we chose it to model the presence of the rigid surfaces, namely

$$U(x,s)=\begin{cases}0, & x>0 \quad \text{and} \quad x+s>0 \quad \text{and} \quad x<D \quad \text{and} \quad D-x-s>0\\ \infty, & \text{elswhere.}\end{cases}$$

This simply assigns an infinitely large energy penalty to any ions not completely residing in the region $0 \leqslant x \leqslant D$.

We assume that the two point-like charges of each rod like ion are connected by an infinitely thin and rigid rod. Therefore these particles do not have excluded volume. But we take into account that the rod-like counterions can not penetrate through the charged surfaces. This is ensured by the external non-electrostatic potential given by $U(x,s)$.

At thermal equilibrium, the free energy $F=F[n(x),\,p(s|x)]$ is minimal with respect to the distributions $n(x)$ and $p(s|x)$, subject to the normalization condition in equation (1). The first variation of the free energy with respect to $n(x)$ and $p(s|x)$ is equal to

$$\begin{aligned}\frac{\delta F}{AkT}=&\int_0^D \mathrm{d}x\,\Psi(x)\frac{\delta\rho(x)}{e}+\int_0^D \mathrm{d}x\,\delta n(x)\ln(\lambda n(x))\\ &+\int_0^D \mathrm{d}x\,\delta n(x)\frac{1}{2l}\int_{-l}^{l}\mathrm{d}s\;p(s|x)\big[\ln p(s|x)+U(x,s)\big]\\ &+\int_0^D \mathrm{d}x\,n(x)\frac{1}{2l}\int_{-l}^{l}\mathrm{d}s\;\delta p(s|x)\big[\ln p(s|x)+1+U(x,s)\big],\end{aligned}\tag{3}$$

where we used the first variation of the Poisson equation $\Psi''(x)=-4\pi l_B\rho(x)/e$. The volume charge density $\rho(x)$ at each position x has two contributions. One expresses the presence of all reference charges that reside at position x with local concentration $n(x)$. The other one accounts for all rod-like ions that have their other charge located at position x. Ions with reference charges in the region $x-l\leqslant s\leqslant x+l$ and an appropriate orientation contribute to this second contribution. Thus,

$$\frac{\rho(x)}{Ze}=n(x)+\frac{1}{2l}\int_{-l}^{l}\mathrm{d}s\,n(x-s)\,p(s|x-s).\tag{4}$$

To carry out the variation $\delta\rho(x)$ in equation (3) we use the equality

$$\int_0^D \mathrm{d}x\frac{1}{2l}\int_{-l}^{l}\mathrm{d}s\;\Psi(x)\delta n(x-s)p(s|x-s)=\int_0^D \mathrm{d}x\frac{1}{2l}\int_{-l}^{l}\mathrm{d}s\;\Psi(x+s)\delta n(x)p(s|x).\tag{5}$$

With this, the variation (3) becomes

$$\begin{aligned}\frac{\delta F}{AkT}=&\int_0^D \mathrm{d}x\frac{1}{2l}\int_{-l}^{l}\mathrm{d}s\big\{n(x)\delta p(s|x)\big[Z\Psi(x+s)+\ln p(s|x)+1+U(x,s)\big]\\ &+\delta n(x)\,p(s|x)\big[Z(\Psi(x)+\Psi(x+s))+\ln[\lambda n(x)\,p(s|x)]+U(x,s)\big]\big\}.\end{aligned}\tag{6}$$

Hence, from the part of equation (6) connected to the variation with respect to $p(s|x)$ we calculate the normalized conditional probability density

$$p(s|x)=\frac{\mathrm{e}^{-U(x,s)-Z\Psi(x+s)}}{\frac{1}{2l}\int_{-l}^{l}\mathrm{d}\bar{s}\;\mathrm{e}^{-U(x,\bar{s})-Z\Psi(x+\bar{s})}}.\tag{7}$$

From the part of equation (6) connected to the variation with respect to $n(x)$ the local concentration of reference charges $n(x)$ of multivalent rod-like counterions can be calculated

$$n(x)=\frac{1}{\lambda}\,\mathrm{e}^{-Z\Psi(x)}\frac{1}{2l}\int_{-l}^{l}\mathrm{d}s\;\mathrm{e}^{-U(x,s)-Z\Psi(x+s)}.\tag{8}$$

If we insert the volume charge density (equation (4); $n(x)$ is given by equation (8) and $p(s|x)$ is given by equation (7)) into the Poisson equation $\Psi''(x) = -4\pi l_B \rho(x)/e$ [39] we obtain the following integral differential equation for the reduced electrostatic potential:

$$\Psi''(x) = -\frac{8\pi l_B Z}{\lambda}\frac{1}{2l}\int_{\max[-l,-x]}^{\min[l,D-x]} ds\, e^{-Z(\Psi(x+s)+\Psi(x))}. \tag{9}$$

Note that the integration limits account for the orientational constraints imposed by the rigid surfaces. Hence, equation (9) is valid in the entire region $0 \leqslant x \leqslant D$. Of course, in the limit $l \to 0$, equation (9) reduces to the familiar nonlinear Poisson–Boltzmann equation for point-like ions $\Psi''(x) = \frac{-8\pi l_B Z}{\lambda} e^{-2Z\Psi(x)}$. The integral differential equation, equation (9), needs to be solved subject to the boundary conditions

$$\Psi'(x=0) = -4\pi l_B \sigma/e \qquad \Psi'(x=D) = 4\pi l_B \sigma/e. \tag{10}$$

Let us remark on two related cases. First, if we add to the solution also negatively charged rod-like coions (with $Z = 1$), then we obtain the following integral differential equation for the reduced electrostatic potential [38]:

$$\Psi''(x) = \frac{\kappa^2}{2}\cdot\frac{1}{2l}\int_{\max[-l,-x]}^{\min[l,D-x]} ds\, \sinh[\Psi(x) + \Psi(x+s)], \tag{11}$$

where $\kappa^2 = 4 \times 8\pi l_B n_0$ and n_0 is the bulk concentration of rod-like counterions and coions. The boundary conditions are given by equations (10).

Second, in the case the solution is composed of rod-like counterions and monovalent salt (positive and negative point-like ions) the integral differential equation becomes

$$\Psi''(x) = -4\pi l_B\left[\frac{2Z}{\lambda}\frac{1}{2l}\int_{\max[-l,-x]}^{\min[l,D-x]} ds\, e^{-Z(\Psi(x+s)+\Psi(x))} + \sum_i i n_{si}\, e^{-i\Psi(x)}\right], \tag{12}$$

where n_{si} is the bulk concentration of the added salt. Again the boundary conditions are given by equations (10).

3. Numerical evaluation of the potential

The integral differential equation, equation (9), with boundary conditions, equation (10), was solved numerically in the following way. The integral differential boundary value problem is restated as a fixed point equation

$$\Psi = \mathcal{F}(\Psi), \tag{13}$$

where $\mathcal{F}(\Psi)$ is the solution Φ of the ordinary differential boundary value problem

$$\Phi''(x) = -8\pi l_B \frac{1}{v_0} Z\, e^{-Z\Phi(x)-2Z\mu}\frac{1}{2l}\int_{\max[-l,l-x]}^{\min[l,D-x]} ds\, e^{-Z\Psi(x+s)} \tag{14a}$$

$$\Phi'(x=0) = -\frac{\sigma e}{\epsilon kT} \tag{14b}$$

$$\Phi'(x=D) = \frac{\sigma e}{\epsilon kT}. \tag{14c}$$

The fixed point equation, equation (13), is discretized by replacing the domain $[0, D]$ of equation (9) by a mesh of N Chebyshev nodes, the function Ψ by an N-dimensional vector Ψ_N of values at the mesh nodes and equation (13) by the finite-dimensional algebraic equation

$$\Psi_N = \pi_N(\mathcal{F}(p_N(\Psi_N))), \tag{15}$$

where $p_N(\Psi_N)$ is the polynomial interpolating the values Ψ_N at the mesh nodes and $\pi_N(\Phi)$ is the N-dimensional vector of the values of the function Φ at the mesh points.

We use MATLAB software for the numerical computation. The discretized fixed point equation, equation (15), is rewritten as

$$G(\Psi_N) = \Psi_N - \pi_N(\mathcal{F}(p_N(\Psi_N))) = 0$$

and then solved by the 'fsolve' MATLAB function (present in the optimization toolbox), which finds solutions of nonlinear algebraic equations by a least square method.

The function 'fsolve' requires the computation of values of G, and so requires the solution of second order ordinary boundary value problems, equations (15). Such problems are restated as first order equations and then solved by the 'bvp4c' MATLAB function, which finds the solution of two-point ordinary boundary value problems by collocation. Finally, the integral in equation (14*a*) is computed by the 'quad' MATLAB function.

3.1. Monte-Carlo simulations

Canonical Monte-Carlo simulations were performed using the integrated Monte-Carlo/molecular dynamic/Brownian dynamic simulation suite Molsim [40] following the standard Metropolis scheme.

Positively charged particles (rod-like counterions) were placed randomly into the Monte-Carlo simulation box. The MC box size was chosen according to the surface charge density of the two surfaces at $x = 0$ and $x = D$ to achieve overall electro-neutrality. One thousand divalent counterions were used. Periodic boundary conditions were applied in both y- and z-directions to mimic an infinite system.

A trial move consists of both a random displacement and a random rotation. Displacement parameters were chosen to obtain about 50% acceptance rate. Thirty thousand attempted moves per particle were used for equilibration followed by 100 000 attempted moves during production runs. Interparticle interactions were calculated as described elsewhere [41], including the contributions from charge distribution outside the MC box. To calculate single particle distributions, the x-axis was divided into 200 bins of width 0.05 nm. The standard deviation of values in histograms was less than 0.2% for each separate bin in all cases.

4. Results

Figure 2 shows the concentration of reference charges $n(x)$ as a function of the distance from the right charged surface x. Different curves correspond to different length l of rod-like counterions. Theoretical results are compared against Monte-Carlo data. Concentration profiles are not smooth even though the potential is smooth due to the orientational restrictions near the charged surface. The inset of figure 2 shows the reduced electrostatic potential $\Psi(x)$ as a function of the distance x from the charged surface.

From the known electrostatic potential the equilibrium electrostatic free energy (equation (2)) can be calculated. Figure 3 shows the electrostatic free energy F/AkT as a function of the distance between two equally charged surfaces D for two different surface charge densities. Figure 3(*A*) shows the calculation for $l = 2$ nm, while figure 3(*B*) shows the calculations for $l = 5$ nm. For small surface charge densities the electrostatic free energy monotonously decreases with increasing distance D. This implies a repulsive force between the two charged surfaces. Quite different behavior is observed for larger surface charge densities and longer ions. Here, the electrostatic free energy adopts a minimum at a finite distance $D = D_{\mathrm{eq}}$. Figure 4 shows the equilibrium distance D_{eq}, where $F(D)$ exhibits an absolute

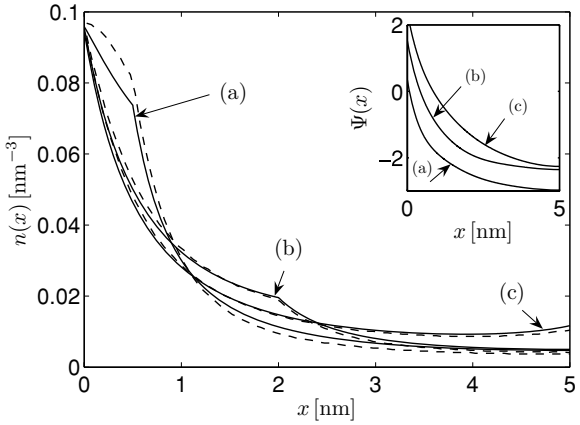

Figure 2. Concentration of reference charges $n(x)$ as a function of x. The different curves correspond to $l = 0.5$ nm (a), $l = 2$ nm (b) and $l = 5$ nm (c). Dashed lines display the theoretical approach whereas full lines display results of MC simulations. The inset shows reduced electrostatic potential $\Psi(x)$ as a function of x. The model parameters are $D = 10$ nm, $Z = 1$ and $\sigma = 0.033$ As m^{-2}.

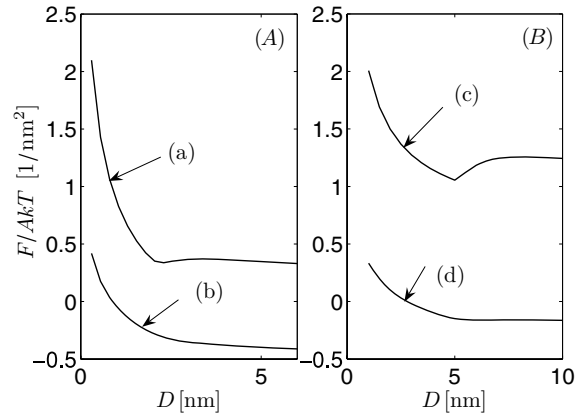

Figure 3. The electrostatic free energy F as a function of the distance between two equally charged surfaces for two different length of rods $l = 2$ nm (A) and $l = 5$ nm (B). The curves (a) and (c) correspond to $\sigma = 0.1$ As m^{-2} while the curves (b) and (d) correspond to $\sigma = 0.033$ As m^{-2}.

minimum, as a function of length of counterions l for four different surface charge densities. The distance D_{eq} increases with increasing l. The critical length of rod-like counterions l_{c} is defined as the minimal length of counterions needed for attractive electrostatic interaction to occur between equally charged surfaces. For example, for $\sigma = 0.1$ As m^{-2} the critical length is $l_{\mathrm{c}} \approx 3$ nm while for $\sigma = 0.033$ As m^{-2} the critical length is $l_{\mathrm{c}} \approx 5$ nm.

The osmotic pressure p due to counterions between two like-charged surface can be evaluated from the contact theorem [42, 43]:

$$\frac{p}{kT} = 2n(0) - \frac{\sigma^2 2\pi l_B}{e^2}, \tag{16}$$

where $n(0)$ is the concentration of reference charges near the charged surface. Figure 5 shows the pressure p as a function of the distance between two charged surfaces for two different

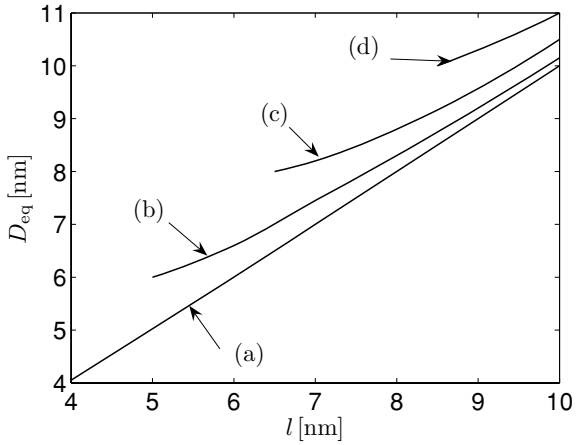

Figure 4. Equilibrium distance D_{eq} as a function of length of rod-like counterions l. The different curves correspond to $\sigma = 0.1$ As m^{-2} (a), $\sigma = 0.033$ As m^{-2} (b), $\sigma = 0.025$ As m^{-2} (c) and $\sigma = 0.02$ As m^{-2} (d).

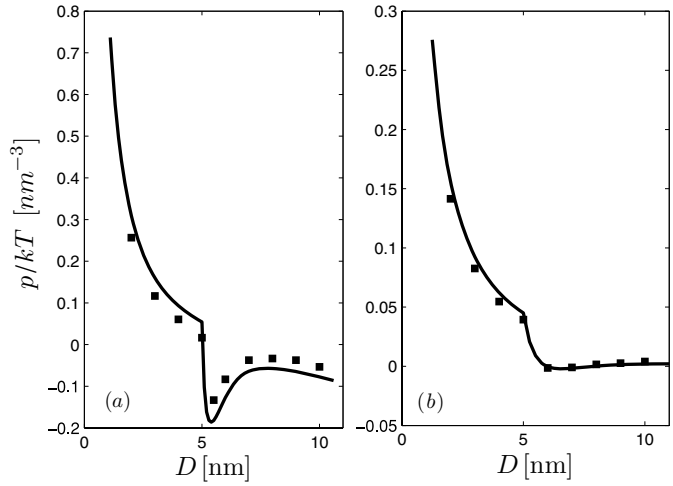

Figure 5. Osmotic pressure p as a function of the distance between the charged surfaces D_{eq}. The full curves correspond to theoretical calculations while the squares correspond to the results of Monte-Carlo simulations. The model parameters are $\sigma = 0.1$ As m^{-2} (a), $\sigma = 0.033$ As m^{-2} (b) and $l = 5$ nm.

surface charge densities. We see that the pressure decreases with increasing distance D. The energetically most favorable situation is at the pressure equal to zero. If we compare figures 3 and 5 we see that the most favorable distance D between the charged surfaces coincides in both cases.

The conditional probability density $p(s|x = 0)$ as a function of the projection s of the rod-like ions with respect to the axis x for two different surface charge densities is shown in figure 6. The reference charge of rod-like counterions is placed near the left charged surface ($x = 0$). In the case $D = l$ (figure 6(A)) the probability density for the second charge of divalent rod-like counterions first decreases with increasing s reaches a minimum and then increases with increasing s. For larger distances between the charged surface (figure 6(B)),

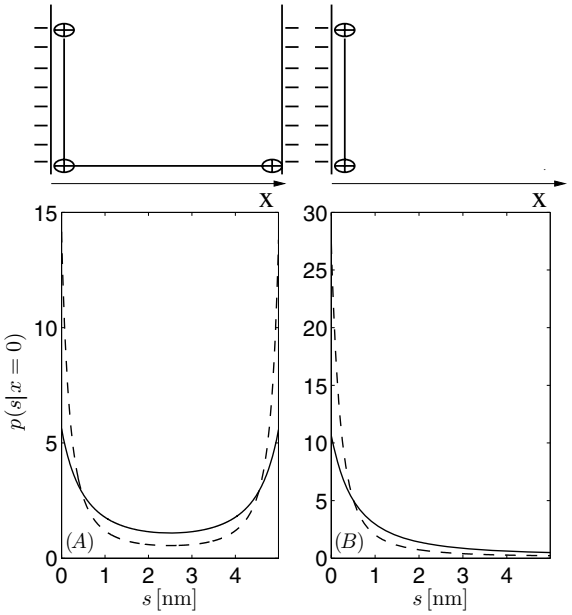

Figure 6. Conditional probability densities $p(s|x = 0)$ as a function of the projection s of the rod-like counterions with respect to the x-axis. The distance between the charged surfaces is $D = 5$ nm (A) and $D = 20$ nm (B). The position of the reference charges was set to $x = 0$. The length of the rod was chosen to $l = 5$ nm. The full lines correspond to $\sigma = 0.033$ As m^{-2} while the dashed lines correspond to $\sigma = 0.1$ As m^{-2}. The schematic presentation of the most probable orientations of rigid rod-like ions with the reference charges located at $x = 0$ (left charged surface) is shown on the top of the figure. In figure (B), the right charged surface is not shown due to large distance D.

the probability $p(s|x = 0)$ monotonously decreases with increasing s. For strongly charged surfaces the variations of $p(s|x = 0)$ with respect to the projection s are much more stronger (see the dashed lines in figure 6).

5. Discussion and conclusion

In the present work, we described a system composed of two equally charged planar surfaces in an electrolyte solution composed of divalent rigid rod-like counterions. For this system we introduced a density functional theory. The theoretical results were checked by the Monte-Carlo simulations. We showed that for sufficiently large surface charge densities and lengths of the divalent rod-like counterions attraction between equally charged surfaces may take place. We also found that the counterions are orientationally ordered.

First we discuss the concentration profiles of reference charges. The concentration of reference charges decreases with increasing distance from the charged surface. The discontinuous derivative of concentration of reference charges $n(x)$ at $x = l$ and $x = D - l$ marks the orientational restriction of counterions close to the charged surface. For divalent rod-like counterions longer than a critical value $l_c^{MC} \approx 1.5$ nm the comparison between the density functional theory and the Monte-Carlo simulations gives a good agreement. Also the non-continuous derivative of the concentration $n(x)$ at $x = l$ and $x = D - l$ is reproduced by Monte-Carlo simulations. In the limit $l \ll l_c^{MC}$ there is a large deviation of the theory from

the Monte-Carlo simulations. The reason for this discrepancy (for short counterions) is the importance of the inter-ionic correlations, which are neglected in our theory. In the limit $l = 0$ the counterions merge to point-like counterions, for which inter-ionic correlations become important.

For long enough couterions there is a good agreement between the theory and the Monte-Carlo simulations because the correlations among different rod-like counterions (inter-ionic correlations) are small and could be neglected. Namely, the correlations between different long rod-like counterions (the two charges of each counterion are spatially separated) can be reduced to the correlations among monovalent charges of different counterions, which are negligible [1]. The electrolyte behaves effectively similar to a monovalent salt. Let us note that in the theory the intra-ionic correlations within a given counterion are taken into account.

Our study was motivated by a number of recent experiments, where the attractive interaction between equally charged macroions mediated by multivalent ions has been observed. The first observation of attraction between two highly negatively charged clays was reported for the $CaCl_2$ solution [12, 44]. Further examples are the network formation in actin solutions induced by divalent ions Ba^{2+} [8], the condensation of DNA induced by three- (four-) valent spermidines (spermines) [4, 5] and the aggregation of viruses induced by divalent diamin ions [9].

We showed that the interaction between two like-charged surfaces in an electrolyte solution composed of multivalent counterions with internal degrees of freedom may be attractive. The attraction is the result of the spatial separation of charges within the multivalent counterions, which evoke the intra-ionic correlations. This intra-ionic correlations are thus incorporated via fixed separation between the charges of rod-like counterions and contribute to the attractive component of the force between equally charged surfaces. Analysis of the orientations of rod-like counterions suggest a bridging mechanism that leads to the stable minimum between the like-charged surfaces. The bridge (rod-like counterions) holds two charged surfaces together (see figure 6). Similarly, an attractive interaction mediated by polymer chains has been observed [45, 46]. This attraction reflects the presence of intra-ionic correlations within the polyelectrolyte. Here we want to stress that intra-ionic correlations can be incorporated into the mean-field electrostatic theory in order to obtain attraction between like-charged planar surfaces.

For large enough surface charge densities and long enough rods the free energy reaches a minimum (figure 3), which corresponds to the energetically most favorable distance D_{eq} between like-charged surfaces. The most favorable distance D_{eq} was confirmed by the osmotic pressure calculations. The osmotic pressure calculations are in good agreement with Monte-Carlo simulations.

We also discuss the conditional probability density (see figure 6). The calculations show that the energetically most favorable distance between the charged surfaces corresponds to the length of the rod-like counterions. At this distance between the surfaces there are two most probable orientations of divalent rod-like counterions: counterions which are oriented parallel and perpendicular to the charged surfaces (see the schematic presentation of orientations in figure 6(A)). Other orientations of rod-like counterions are less pronounced. The parallel and perpendicular orientations indicate the tendency of counterion charges to be in contact with the negatively charged surface. For high surface charge densities both preferred orientations are even pronounced. The counterions which are oriented perpendicular to the charged surfaces connect both surfaces and act as a bridge between equally charged surfaces. This bridging mechanism of rod-like charged counterions is responsible for the attractive interaction between like-charged surfaces [47, 48]. At larger separations between the charged surfaces, the most

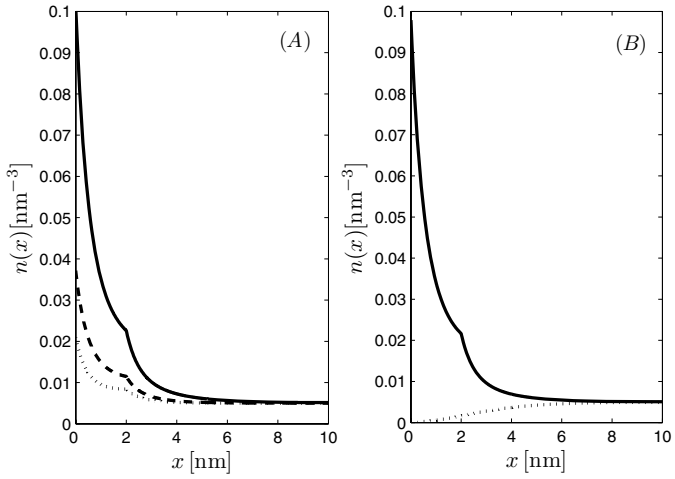

Figure 7. Concentration of rod-like ions as a function of x. (A) Rod-like counterions with added monovalent salt of bulk concentrations 0 mol $\cdot$ l^{-1} (full line), 0.05 mol $\cdot$ l^{-1} (dashed line) and 0.1 mol $\cdot$ l^{-1} (dotted line). (B) The system of rod-like counterions and coions with the bulk concentrations of 0.005 nm^{-3}. The model parameters are the length of the rods $l = 2$ nm, the surface charge density $\sigma = 0.033$ As m^{-2} and the distance between the charged surfaces $D = 20$ nm.

probable orientations of rigid rod-like ions are those parallel to the charged surfaces and no bridging occurs (see the schematic presentation of orientations in figure 6(B)).

In our model we adopted some simplifications. First we did not take into account the excluded volume of rod-like ions. Second the correlations between different rod-like ions were not taken into account. Third we did not consider the partial adsorption of rod-like counterions on the charged surface. Fourth, we assumed uniformly distributed charge on the surfaces.

The multivalent rod-like ions possess an electric quadrupole moment which orders in the electric field gradient of the system (charged surfaces and solution). This quadrupolar ordering is stronger for higher surface charge densities. For large enough surface charge densities the quadrupolar ordering of long rigid rod-like counterions gives rise to the attractive force between like-charged surfaces.

We can state that the attraction between equally charged surfaces takes place above a critical length of rod-like counterions and above a critical surface charge density. If attraction is found, the equilibrium distance between equally charged surfaces increases with increasing length of the rod-like counterions. Larger surface charge densities increase the strength of the electrostatic interaction leading to smaller optimal distances between the charged surfaces and smaller critical length l_c.

The addition of monovalent salt into the solution composed of rod-like counterions has large influence on the concentration profile of rod-like counterions close to the charged surface (figure 7(A)). The increasing salt concentration decreases the concentration of rod-like counterions close to the charged surface. The reason for this decrease is the screening of the surface charge by monovalent counterions. This behavior also has influence on the attraction between like-charged surfaces. The increasing salt concentration decreases the free energy barrier for the attractive interaction. Again the reason for this effect is screening of charges on the charged surfaces by counterions of the solution.

We also studied the system composed of rod-like counterions and coions (figure 7(*B*)). First we note that the overall concentration of coions in the slit is much smaller than the overall concentration of counterions. With increasing surface charge density the concentration of coions becomes negligibly small compared with the concentration of counterions. With decreasing distance between the charged surfaces the concentration of rod-like coions becomes negligible. The rod-like coions have very small influence on the interaction between equally charged surfaces.

In summary, we considered two equally charged surfaces which are filled with an aqueous solution of rigid divalent rod-like counterions. The variational minimization applied to the free energy leads to an integral differential equation, which was solved numerically. We calculated the free energy of the system and the osmotic pressure between like-charged surfaces. The numerical results have been verified by Monte-Carlo simulations. It was shown that for long enough divalent rod-like counterions the theoretical results are in good agreement with Monte-Carlo simulations. We found attractive interaction between highly like-charged surfaces due to orientational ordering of rigid long divalent rod-like counterions.

Acknowledgments

This work was supported by the Slovenian Research Agency through the Physical Chemistry Research Program 0103-0201, Research Project J1-6653. The authors thank Professor Bo Jönsson for the helpful discussion. SM acknowledges support from NSF through DMR-0605883.

References

[1] Evans D F and Wennerström H 1994 *The Colloidal Domain, Where Physics, Chemistry, Biology and Technology Meet* (New York: VCH)
[2] Hribar B and Vlachy V 1997 *J. Phys. Chem.* B **101** 3457
[3] Linse P 2000 *J. Chem. Phys.* **113** 4359
[4] Bloomfield V A 1996 *Curr. Opin. Struct. Biol.* **6** 334
[5] Teif V 2005 *Biophys. J.* **89** 2574
[6] Rädler J O, Koltover I, Salditt T and Safinya C R 1997 *Science* **275** 810
[7] Gelbart W M, Bruinsma R, Pincus P A and Parsegian V A 2000 *Phys. Today* **53** 38
[8] Angelini T E, Liang H, Wriggers W and Wong G C L 2003 *Proc. Natl. Acad. Sci. USA* **100** 8634
[9] Butler J C, Angelini T, Tang J X and Wong G C L 2003 *Phys. Rev. Lett.* **91** 028301
[10] Khan A, Fontell K and Lindman B 1984 *J. Colloid Interface Sci.* **101** 193
[11] Wennerström H, Khan A and Lindman B 1991 *Adv. Colloid Interface Sci.* **34** 433
[12] Kjellander R, Marčelja S, Pashley R M and Quirk J P 1988 *J. Phys. Chem.* **92** 6489
[13] Safran S A 2003 *Statistical Thermodynamics of Surfaces, Interfaces, and Membranes* (Colorado: Westview Press)
[14] Carnie S and McLaughlin S 1983 *Biophys. J.* **44** 325
[15] Kirkwood J K and Shumaker J B 1952 *Proc. Natl. Acad. Sci. USA* **38** 863
[16] Oosawa F 1968 *Biopolymers* **6** 1633
[17] Guldbrand L, Jönsson B, Wennerström H and Linse P 1984 *J. Chem. Phys.* **80** 2221
[18] Svensson B and Jönsson B 1984 *Chem. Phys. Lett.* **108** 580
[19] Moreira A G and Netz R R 2001 *Phys. Rev. Lett.* **87** 078301
[20] Reščič J and Linse P 2000 *J. Phys. Chem.* B **104** 7852
[21] Grosberg A Y, Nguyen T T and Shklovskii B I 2002 *Rev. Mod. Phys.* **74** 329
[22] Netz R R 2001 *Eur. Phys. J.* E **5** 557
[23] Levin Y 2002 *Rep. Prog. Phys.* **65** 1577
[24] Kjellander R and Marčelja S 1988 *J. Phys. France* **49** 1009
[25] Kjellander R 1996 *Ber. Bunsenges. Phys. Chem.* **100** 894
[26] Lozada-Cassou M and Diaz-Herrera E 1990 *J. Chem. Phys.* **93** 1386

[27] Rouzina I and Bloomfeld V A 1996 *J. Phys. Chem.* **100** 9977
[28] Linse P 2002 *J. Phys.: Condens. Matter.* **14** 13449
[29] Åkesson T, Woodward C and Jönsson B 1989 *J. Chem. Phys.* **91** 2461
[30] Miklavic S J, Woodward C E, Jönsson B and Åkesson T 1990 *Macromolecules* **23** 4149
[31] Podgornik R, Åkesson T and Jönsson B 1995 *J. Chem. Phys.* **102** 9423
[32] Woodward C E, Åkesson T and Jönsson B 1994 *J. Chem. Phys.* **101** 2569
[33] Akinchina A and Linse P 2003 *J. Phys. Chem.* B **107** 8011
[34] Turesson M, Forsman J and Åkesson T 2006 *Langmuir* **22** 5734
[35] Bohinc K, Iglič A and May S 2004 *Europhys. Lett.* **68** 494
[36] Maset S and Bohinc K 2007 *J. Phys. A: Math. Theor.* **40** 11815
[37] Kim Y W, Yi J and Pincus P A 2008 *Phys. Rev. Lett.* **101** 208305
[38] May S, Iglič A, Reščič J, Maset S and Bohinc K 2008 *J. Chem. Phys.* B **112** 1685
[39] Jackson J D 1998 *Classical Electrodynamics* (New York: John Wiley & Sons)
[40] Linse P 2006 *Molsim 4.1.7* Lund University, Sweden
[41] Jönsson B, Wennerström H and Halle B 1990 *J. Phys. Chem.* **84** 2179
[42] Henderson D and Blum L 1978 *J. Chem. Phys.* **69** 5441
[43] Henderson D, Blum L and Lebowitz J L 1979 *J. Electroanal. Chem.* **102** 315
[44] Marra J 1986 *Biophys. J.* **50** 815
[45] Borukhov I, Andelman D and Orland H 1999 *J. Phys. Chem.* **103** 5042
[46] Allen R J and Warren P B 2004 *Langmuir* **20** 1997
[47] Urbanija J, Bohinc K, Bellen A, Maset S, Iglič A, Kralj-Iglič V and Sunil P B S 2008 *J. Chem. Phys.* **129** 105101
[48] Podgornik R 2004 *J. Polym. Sci.* B *(Polym. Phys.)* **42** 3539